PHYSICAL REVIEW D **86,** 031102(R) (2012)

# Observation of exclusive $\Upsilon(1S)$ and $\Upsilon(2S)$ decays into light hadrons

C. P. Shen,[29] C. Z. Yuan,[13] T. Iijima,[30,29] I. Adachi,[10] H. Aihara,[51] D. M. Asner,[39] T. Aushev,[16] A. M. Bakich,[45] A. Bay,[23] K. Belous,[15] B. Bhuyan,[11] M. Bischofberger,[31] G. Bonvicini,[56] A. Bozek,[35] M. Bračko,[26,17] T. E. Browder,[9] M.-C. Chang,[5] P. Chang,[34] A. Chen,[32] P. Chen,[34] B. G. Cheon,[8] K. Chilikin,[16] R. Chistov,[16] I.-S. Cho,[58] K. Cho,[20] S.-K. Choi,[7] Y. Choi,[44] J. Dalseno,[27,47] Z. Doležal,[3] Z. Drásal,[3] S. Eidelman,[2] J. E. Fast,[39] V. Gaur,[46] N. Gabyshev,[2] Y. M. Goh,[8] B. Golob,[24,17] J. Haba,[10] H. Hayashii,[31] Y. Horii,[30] Y. Hoshi,[49] W.-S. Hou,[34] Y. B. Hsiung,[34] H. J. Hyun,[22] K. Inami,[29] A. Ishikawa,[50] R. Itoh,[10] M. Iwabuchi,[58] Y. Iwasaki,[10] T. Iwashita,[31] T. Julius,[28] J. H. Kang,[58] T. Kawasaki,[37] C. Kiesling,[27] B. H. Kim,[43] H. O. Kim,[22] J. B. Kim,[21] J. H. Kim,[20] M. J. Kim,[22] Y. J. Kim,[20] K. Kinoshita,[4] B. R. Ko,[21] S. Koblitz,[27] P. Kodyš,[3] S. Korpar,[26,17] R. T. Kouzes,[39] P. Križan,[24,17] P. Krokovny,[2] R. Kumar,[40] T. Kumita,[53] A. Kuzmin,[2] Y.-J. Kwon,[58] S.-H. Lee,[21] J. Li,[43] Y. Li,[55] J. Libby,[12] C. Liu,[42] Y. Liu,[4] Z. Q. Liu,[13] R. Louvot,[23] S. McOnie,[45] K. Miyabayashi,[31] H. Miyata,[37] G. B. Mohanty,[46] D. Mohapatra,[39] A. Moll,[27,47] N. Muramatsu,[41] E. Nakano,[38] M. Nakao,[10] Z. Natkaniec,[35] S. Nishida,[10] K. Nishimura,[9] O. Nitoh,[54] S. Ogawa,[48] T. Ohshima,[29] S. Okuno,[18] S. L. Olsen,[43,9] P. Pakhlov,[16] G. Pakhlova,[16] C. W. Park,[44] H. Park,[22] H. K. Park,[22] T. K. Pedlar,[25] R. Pestotnik,[17] M. Petrič,[17] L. E. Piilonen,[55] M. Ritter,[27] H. Sahoo,[9] Y. Sakai,[10] D. Santel,[4] T. Sanuki,[50] Y. Sato,[50] O. Schneider,[23] C. Schwanda,[14] K. Senyo,[57] O. Seon,[29] M. E. Sevior,[28] M. Shapkin,[15] V. Shebalin,[2] T.-A. Shibata,[52] J.-G. Shiu,[34] B. Shwartz,[2] A. Sibidanov,[45] F. Simon,[27,47] P. Smerkol,[17] Y.-S. Sohn,[58] A. Sokolov,[15] E. Solovieva,[16] M. Starič,[17] M. Sumihama,[6] T. Sumiyoshi,[53] G. Tatishvili,[39] Y. Teramoto,[38] M. Uchida,[52] S. Uehara,[10] T. Uglov,[16] Y. Unno,[8] S. Uno,[10] P. Urquijo,[1] Y. Usov,[2] P. Vanhoefer,[27] G. Varner,[9] C. H. Wang,[33] P. Wang,[13] X. L. Wang,[13] M. Watanabe,[37] Y. Watanabe,[18] K. M. Williams,[55] E. Won,[21] B. D. Yabsley,[45] Y. Yamashita,[36] C. C. Zhang,[13] Z. P. Zhang,[42] V. Zhilich,[2] V. Zhulanov,[2] and A. Zupanc[19]

(The Belle Collaboration)

[1]*University of Bonn, Bonn*
[2]*Budker Institute of Nuclear Physics SB RAS and Novosibirsk State University, Novosibirsk 630090*
[3]*Faculty of Mathematics and Physics, Charles University, Prague*
[4]*University of Cincinnati, Cincinnati, Ohio 45221*
[5]*Department of Physics, Fu Jen Catholic University, Taipei*
[6]*Gifu University, Gifu*
[7]*Gyeongsang National University, Chinju*
[8]*Hanyang University, Seoul*
[9]*University of Hawaii, Honolulu, Hawaii 96822*
[10]*High Energy Accelerator Research Organization (KEK), Tsukuba*
[11]*Indian Institute of Technology Guwahati, Guwahati*
[12]*Indian Institute of Technology Madras, Madras*
[13]*Institute of High Energy Physics, Chinese Academy of Sciences, Beijing*
[14]*Institute of High Energy Physics, Vienna*
[15]*Institute of High Energy Physics, Protvino*
[16]*Institute for Theoretical and Experimental Physics, Moscow*
[17]*J. Stefan Institute, Ljubljana*
[18]*Kanagawa University, Yokohama*
[19]*Institut für Experimentelle Kernphysik, Karlsruher Institut für Technologie, Karlsruhe*
[20]*Korea Institute of Science and Technology Information, Daejeon*
[21]*Korea University, Seoul*
[22]*Kyungpook National University, Taegu*
[23]*École Polytechnique Fédérale de Lausanne (EPFL), Lausanne*
[24]*Faculty of Mathematics and Physics, University of Ljubljana, Ljubljana*
[25]*Luther College, Decorah, Iowa 52101*
[26]*University of Maribor, Maribor*
[27]*Max-Planck-Institut für Physik, München*
[28]*University of Melbourne, School of Physics, Victoria 3010*
[29]*Graduate School of Science, Nagoya University, Nagoya*
[30]*Kobayashi-Maskawa Institute, Nagoya University, Nagoya*
[31]*Nara Women's University, Nara*
[32]*National Central University, Chung-li*
[33]*National United University, Miao Li*

 

[34]*Department of Physics, National Taiwan University, Taipei*
[35]*H. Niewodniczanski Institute of Nuclear Physics, Krakow*
[36]*Nippon Dental University, Niigata*
[37]*Niigata University, Niigata*
[38]*Osaka City University, Osaka*
[39]*Pacific Northwest National Laboratory, Richland, Washington 99352*
[40]*Panjab University, Chandigarh*
[41]*Research Center for Electron Photon Science, Tohoku University, Sendai*
[42]*University of Science and Technology of China, Hefei*
[43]*Seoul National University, Seoul*
[44]*Sungkyunkwan University, Suwon*
[45]*School of Physics, University of Sydney, NSW 2006*
[46]*Tata Institute of Fundamental Research, Mumbai*
[47]*Excellence Cluster Universe, Technische Universität München, Garching*
[48]*Toho University, Funabashi*
[49]*Tohoku Gakuin University, Tagajo*
[50]*Tohoku University, Sendai*
[51]*Department of Physics, University of Tokyo, Tokyo*
[52]*Tokyo Institute of Technology, Tokyo*
[53]*Tokyo Metropolitan University, Tokyo*
[54]*Tokyo University of Agriculture and Technology, Tokyo*
[55]*CNP, Virginia Polytechnic Institute and State University, Blacksburg, Virginia 24061*
[56]*Wayne State University, Detroit, Michigan 48202*
[57]*Yamagata University, Yamagata*
[58]*Yonsei University, Seoul*

(Received 6 May 2012; published 15 August 2012)

Using samples of $102 \times 10^6$ $\Upsilon(1S)$ and $158 \times 10^6$ $\Upsilon(2S)$ events collected with the Belle detector, we study exclusive hadronic decays of these two bottomonium resonances to the three-body final states $\phi K^+ K^-$, $\omega \pi^+ \pi^-$ and $K^{*0}(892) K^- \pi^+$, and to the two-body Vector-Tensor states ($\phi f_2'(1525)$, $\omega f_2(1270)$, $\rho a_2(1320)$ and $K^{*0}(892)\bar{K}_2^{*0}(1430)$) and Axial-vector-Pseudoscalar ($K_1(1270)^+ K^-$, $K_1(1400)^+ K^-$ and $b_1(1235)^+ \pi^-$) states. Signals are observed for the first time in the $\Upsilon(1S) \to \phi K^+ K^-$, $\omega \pi^+ \pi^-$, $K^{*0} K^- \pi^+$, $K^{*0} K_2^{*0}$ and $\Upsilon(2S) \to \phi K^+ K^-$, $K^{*0} K^- \pi^+$ decay modes. Branching fractions are determined for all the processes, while 90% confidence level upper limits are established on the branching fractions for the modes with a statistical significance less than $3\sigma$. The ratios of the branching fractions of $\Upsilon(2S)$ and $\Upsilon(1S)$ decays into the same final state are used to test a perturbative QCD prediction for OZI-suppressed bottomonium decays.

DOI: 10.1103/PhysRevD.86.031102 PACS numbers: 13.25.Gv, 12.38.Qk, 14.40.Pq

Although around 80% of the $\Upsilon(1S)$ decays and 60% of the $\Upsilon(2S)$ decays are expected to result in hadronic final states via annihilation into gluons [1,2], no single exclusive mode has been reported [3]. This situation is quite different from the charmonium sector, where numerous channels have been measured and used to test a variety of theoretical models. The OZI (Okubo-Zweig-Iizuka) [4] suppressed decays of the $J/\psi$ and $\psi(2S)$ to hadrons proceed via the annihilation of the quark-antiquark pair into three gluons or a photon. For both cases, perturbative quantum chromodynamics (pQCD) provides a relation for the ratios of branching fractions ($\mathcal{B}$) for $J/\psi$ and $\psi(2S)$ decays [5]

$$Q_\psi = \frac{\mathcal{B}_{\psi(2S)\to\text{hadrons}}}{\mathcal{B}_{J/\psi\to\text{hadrons}}} = \frac{\mathcal{B}_{\psi(2S)\to e^+e^-}}{\mathcal{B}_{J/\psi\to e^+e^-}} \approx 12\%, \quad (1)$$

which is referred to as the "12% rule" and is expected to apply with reasonable accuracy to both inclusive and exclusive decays. However, it is found to be severely violated for $\rho\pi$ and other Vector-Pseudoscalar ($VP$) and Vector-Tensor ($VT$) final states. None of the many existing theoretical explanations that have been proposed have been able to accommodate all the measurements reported to date [6].

A similar rule can be derived for OZI-suppressed bottomonium decays, in which case we expect

$$Q_\Upsilon = \frac{\mathcal{B}_{\Upsilon(2S)\to\text{hadrons}}}{\mathcal{B}_{\Upsilon(1S)\to\text{hadrons}}} = \frac{\mathcal{B}_{\Upsilon(2S)\to e^+e^-}}{\mathcal{B}_{\Upsilon(1S)\to e^+e^-}} = 0.77 \pm 0.07. \quad (2)$$

This rule should hold better than the 12% rule for charmonium decay, since the bottomonium states have higher mass, pQCD and the potential models should be more applicable, as has been demonstrated in calculations of the $b\bar{b}$ meson spectrum.

In this Letter, we report studies of exclusive hadronic decays of the $\Upsilon(1S)$ and $\Upsilon(2S)$ resonances to the three-body final states $\phi K^+ K^-$, $\omega \pi^+ \pi^-$, and $K^{*0}(892) K^- \pi^+$

[7] and two-body $VT$ [$\phi f_2'(1525) \to \phi K^+K^-$, $\omega f_2(1270) \to \omega\pi^+\pi^-$, $\rho a_2(1320) \to \rho^0\rho^+\pi^-$, and $K^{*0}(892)\bar{K}_2^{*0}(1430) \to K^{*0}(892)K^-\pi^+$] and Axial-vector-Pseudoscalar ($AP$) [$K_1(1270)^+K^- \to \rho^0K^+K^-$, $K_1(1400)^+K^- \to K^{*0}(892)\pi^+K^-$, and $b_1(1235)^+\pi^- \to \omega\pi^+\pi^-$] final states. This analysis is based on a 5.7 fb$^{-1}$ $\Upsilon(1S)$ data sample ($102 \times 10^6$ $\Upsilon(1S)$ events), a 24.7 fb$^{-1}$ $\Upsilon(2S)$ data sample ($158 \times 10^6$ $\Upsilon(2S)$ events), and a 89.4 fb$^{-1}$ continuum data sample collected at $\sqrt{s} = 10.52$ GeV. Here, $\sqrt{s}$ is the center-of-mass (C.M.) energy of the colliding $e^+e^-$ system. The data are collected with the Belle detector [8] operating at the KEKB asymmetric-energy $e^+e^-$ collider [9]. The EVTGEN [10] generator is used to simulate Monte Carlo (MC) events. For two-body decays, the angular distributions are generated using the formulae in Ref. [11]. Inclusive $\Upsilon(1S)$ and $\Upsilon(2S)$ MC events, produced using PYTHIA [12] with the same luminosity as real data, are used to check for possible peaking backgrounds.

We require four reconstructed charged tracks with zero net charge. For these tracks, the impact parameters perpendicular to and along the beam direction with respect to the interaction point are required to be less than 0.5 cm and 4 cm, respectively, and the transverse momentum in the laboratory frame is restricted to be higher than 0.1 GeV/$c$. For each charged track, we combine information from different detector subsystems to form a likelihood $\mathcal{L}_i$ for each particle species [13].

A track with $\mathcal{R}_K = \frac{\mathcal{L}_K}{\mathcal{L}_K + \mathcal{L}_\pi} > 0.6$ is identified as a kaon, while a track with $\mathcal{R}_K < 0.4$ is treated as a pion. With this selection, the kaon (pion) identification efficiency is about 89% (92%), while 6% (9%) of kaons (pions) are misidentified as pions (kaons). A similar likelihood ratio $\mathcal{R}_\mu$ is formed for muon identification [14]. Except for the $\phi K^+K^-$ final state for which at least three charged tracks are required to be identified as kaons, all other charged tracks are required to be positively identified as pions or kaons. A small background with muons is removed by requiring $\mathcal{R}_\mu < 0.95$ for the pion candidates.

A neutral cluster in the electromagnetic calorimeter is reconstructed as a photon, if it does not match the extrapolated position of any charged track and its energy is greater than 40 MeV. A $\pi^0$ candidate is reconstructed from a pair of photons. We perform a mass-constrained fit to the selected $\pi^0$ candidate and require $\chi^2 < 6$.

We impose an energy conservation requirement on $X_T = \Sigma_h E_h/\sqrt{s}$, where $E_h$ is the energy of the final-state particle $h$ in the $e^+e^-$ C.M. frame. The ratio $X_T$ should lie in the range $0.985 \le X_T \le 1.015$ for channels with a $\pi^0$ in the final state, and in the range $0.99 \le X_T \le 1.01$ for other channels. Figure 1 shows the $X_T$ distributions from $\Upsilon(1S)$ and $\Upsilon(2S)$ decays to $\phi K^+K^-$, $\omega\pi^+\pi^-$ and $K^{*0}(892)$

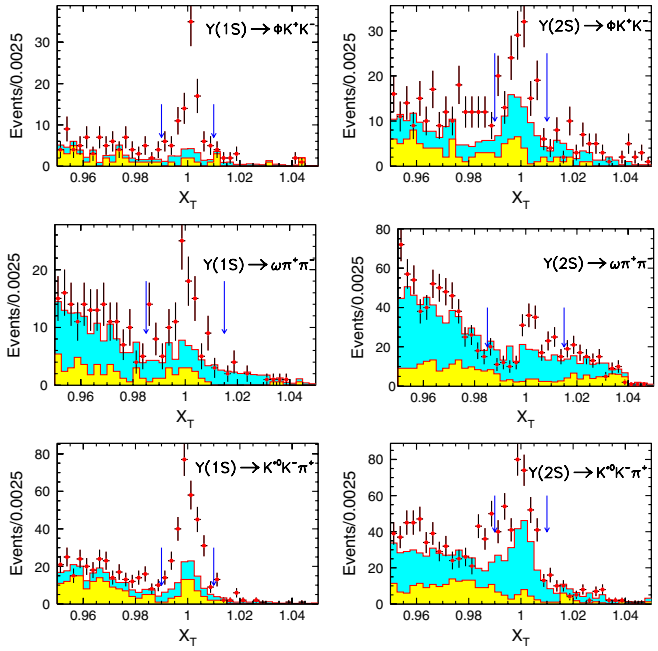


FIG. 1 (color online). Scaled total energy, $X_T$, distributions from $\Upsilon(1S)$ and $\Upsilon(2S)$ decays to $\phi K^+K^-$, $\omega\pi^+\pi^-$ and $K^{*0}(892)K^-\pi^+$. The dots with error bars are from resonance data; the dark-shaded histograms are from normalized continuum contributions; the light-shaded histograms are from inclusive $\Upsilon(1S)$ and $\Upsilon(2S)$ MC events with signals removed. The arrows show the required signal region.

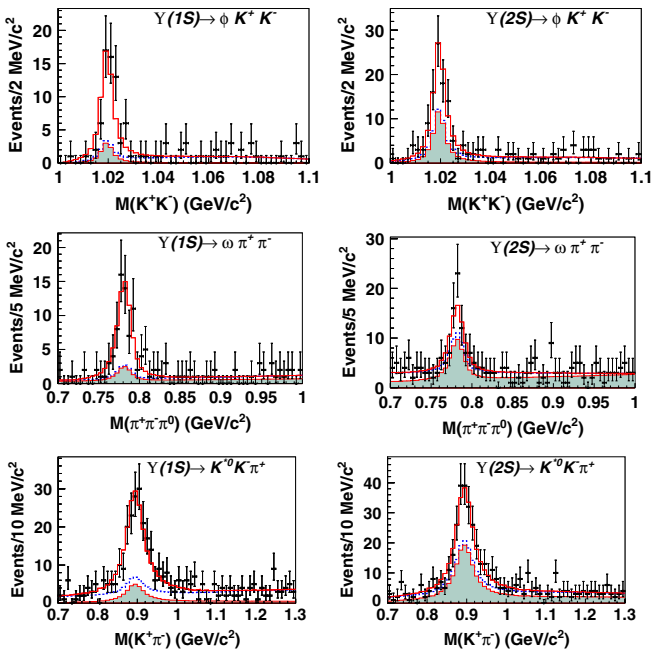


FIG. 2 (color online). The $K^+K^-$ (top row), $\pi^+\pi^-\pi^0$ (middle row), and $K^+\pi^-$ (bottom row) invariant-mass distributions for the final candidate events from $\Upsilon(1S)$ (left column) and $\Upsilon(2S)$ (right column) three-body decays. Solid points with error bars are data, open histograms show the best fits, dashed curves are the total background estimates, and shaded histograms are the normalized continuum background contributions.

TABLE I. Results for the $\Upsilon(1S)$ and $\Upsilon(2S)$ decays, where $N^{\rm sig}$ is the number of fitted signal events, $N^{\rm UP}_{\rm sig}$ is the upper limit on the number of signal events, $\epsilon$ is the efficiency (%), $\Sigma$ is the statistical significance ($\sigma$), $\mathcal{B}$ is the branching fraction, $\mathcal{B}^{\rm UP}$ is the upper limit on the branching fraction, $\mathcal{Q}_\Upsilon$ is the ratio of the $\Upsilon(2S)$ and $\Upsilon(1S)$ branching fractions, and $\mathcal{Q}^{\rm UP}_\Upsilon$ is the upper limit on the value of $\mathcal{Q}_\Upsilon$. Branching fractions are in units of $10^{-6}$ and upper limits are given at the 90% C.L. The first error in $\mathcal{B}$ and $\mathcal{Q}_\Upsilon$ is statistical, and the second systematic.

| Channel | $\Upsilon$ (1S) | | | | | $\Upsilon$ (2S) | | | | | | |
|---|---|---|---|---|---|---|---|---|---|---|---|---|
| | $N^{\rm sig}$ | $N^{\rm UP}_{\rm sig}$ | $\epsilon$ | $\Sigma$ | $\mathcal{B}$ | $\mathcal{B}^{\rm UP}$ | $N^{\rm sig}$ | $N^{\rm UP}_{\rm sig}$ | $\epsilon$ | $\Sigma$ | $\mathcal{B}$ | $\mathcal{B}^{\rm UP}$ | $\mathcal{Q}_\Upsilon$ | $\mathcal{Q}^{\rm UP}_\Upsilon$ |
| $\phi K^+K^-$ | $56.3 \pm 8.7$ | | 47.9 | 8.6 | $2.36 \pm 0.37 \pm 0.29$ | | $58 \pm 12$ | | 47.8 | 6.5 | $1.58 \pm 0.33 \pm 0.18$ | | $0.67 \pm 0.18 \pm 0.11$ | |
| $\omega\pi^+\pi^-$ | $63.6 \pm 9.5$ | | 15.7 | 8.5 | $4.46 \pm 0.67 \pm 0.72$ | | $29 \pm 12$ | 51 | 15.9 | 2.5 | $1.32 \pm 0.54 \pm 0.45$ | 2.58 | $0.30 \pm 0.13 \pm 0.11$ | 0.55 |
| $K^{*0}K^-\pi^+$ | $173 \pm 20$ | | 28.7 | 11 | $4.42 \pm 0.50 \pm 0.58$ | | $135 \pm 23$ | | 27.5 | 6.4 | $2.32 \pm 0.40 \pm 0.54$ | | $0.52 \pm 0.11 \pm 0.14$ | |
| $\phi f_2'$ | $6.9 \pm 3.9$ | 15 | 48.8 | 2.1 | $0.64 \pm 0.37 \pm 0.14$ | 1.63 | $8.3 \pm 6.0$ | 18 | 49.0 | 1.6 | $0.50 \pm 0.36 \pm 0.19$ | 1.33 | $0.77 \pm 0.70 \pm 0.33$ | 2.54 |
| $\omega f_2$ | $5.2 \pm 4.0$ | 13 | 17.7 | 1.5 | $0.57 \pm 0.44 \pm 0.13$ | 1.79 | $-0.4 \pm 3.3$ | 6.1 | 17.5 | | $-0.03 \pm 0.24 \pm 0.01$ | 0.57 | $-0.06 \pm 0.42 \pm 0.02$ | 1.22 |
| $\rho a_2$ | $29 \pm 11$ | 49 | 17.4 | 2.7 | $1.15 \pm 0.47 \pm 0.18$ | 2.24 | $10 \pm 11$ | 30 | 17.3 | 0.9 | $0.27 \pm 0.28 \pm 0.14$ | 0.88 | $0.23 \pm 0.26 \pm 0.12$ | 0.82 |
| $K^{*0}\bar{K}_2^{*0}$ | $42.2 \pm 9.5$ | | 30.8 | 5.4 | $3.02 \pm 0.68 \pm 0.34$ | | $32 \pm 11$ | | 29.6 | 3.3 | $1.53 \pm 0.52 \pm 0.19$ | | $0.50 \pm 0.21 \pm 0.07$ | |
| $K_1(1270)^+K^-$ | $3.7 \pm 4.9$ | 13 | 23.6 | 0.8 | $0.54 \pm 0.72 \pm 0.21$ | 2.41 | $11.0 \pm 4.4$ | 26 | 23.5 | 1.2 | $1.06 \pm 0.42 \pm 0.32$ | 3.22 | $1.96 \pm 2.71 \pm 0.84$ | 4.73 |
| $K_1(1400)^+K^-$ | $23.8 \pm 8.2$ | | 27.3 | 3.3 | $1.02 \pm 0.35 \pm 0.22$ | | $9.2 \pm 8.2$ | 24 | 26.9 | 0.5 | $0.26 \pm 0.23 \pm 0.09$ | 0.83 | $0.26 \pm 0.25 \pm 0.10$ | 0.77 |
| $b_1(1235)^+\pi^-$ | $14.4 \pm 6.9$ | 28 | 16.7 | 2.4 | $0.47 \pm 0.22 \pm 0.13$ | 1.25 | $1.2 \pm 3.5$ | 13 | 17.0 | 0.2 | $0.02 \pm 0.07 \pm 0.01$ | 0.40 | $0.05 \pm 0.16 \pm 0.03$ | 0.35 |

$K^-\pi^+$, together with expected backgrounds from continuum processes and $\Upsilon$(1S) and $\Upsilon$(2S) decays. Obvious signal candidates at $X_T \sim 1$ can be seen.

For three-body decay modes with a $\phi$ or $\omega$, $\phi$ ($\omega$) candidates are selected with $K^+K^-$ ($\pi^+\pi^-\pi^0$) masses closest to the nominal $\phi$ ($\omega$) mass [1]. Figure 2 shows the $K^+K^-$, $\pi^+\pi^-\pi^0$, and $K^+\pi^-$ invariant-mass distributions for $\Upsilon(1S)$ and $\Upsilon(2S)$ to $\phi K^+K^-$, $\omega\pi^+\pi^-$ and $K^{*0}(892)$ $K^-\pi^+$ candidates that survive the selection criteria described above. Clear $\phi$, $\omega$, and $K^{*0}(892)$ signals are evident.

After the application of all of the selection requirements, no peaking backgrounds from the $\Upsilon(1S)$ and $\Upsilon(2S)$ inclusive MC samples are found in the vector meson mass regions. Potential backgrounds due to particle misidentification, from $\phi\pi^+\pi^-$ for example, are estimated by selecting these events in the data and normalizing them using measured misidentification probabilities. Potential backgrounds from events with additional $\pi^0$'s are checked by examining the recoil mass distribution from the measured final state. For $\omega\pi^+\pi^-$, potential background events from $\omega\eta'$ with $\eta' \to \gamma\pi^+\pi^-$ are explicitly reconstructed from data and estimated using $N\epsilon_1/\epsilon_2$, where $N$ is the number of $\omega\eta'$ events in data and $\epsilon_1$ and $\epsilon_2$ are the efficiencies after the $\omega\pi^+\pi^-$ and $\omega\eta'$ event selections, respectively. All of the above backgrounds are found to be negligibly small. For $\omega\pi^+\pi^-$, the fraction of events with multiple combinations is at the 3.5% level due to multiple $\pi^0$ candidates; this is consistent with the MC simulation and is taken into account in the efficiency determination.

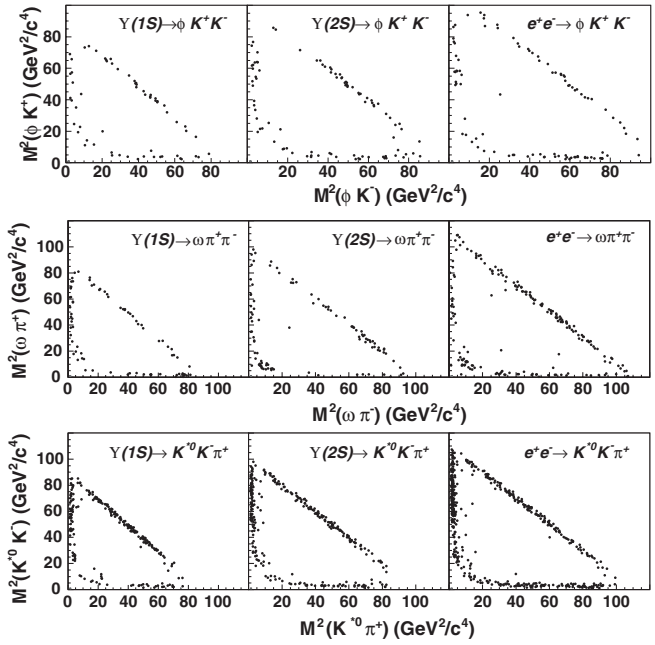


FIG. 3. Dalitz plots of $\phi K^+K^-$ (top row), $\omega\pi^+\pi^-$ (middle row) and $K^{*0}(892)K^-\pi^+$ (bottom row) three-body final states. Here, the left column is for $\Upsilon(1S)$ decays, the middle column is for $\Upsilon(2S)$ decays, and the right column is for the continuum data.

The continuum background contribution is determined from the data at $\sqrt{s} = 10.52$ GeV and is extrapolated down to the $\Upsilon(1S)$ and $\Upsilon(2S)$ resonances. For the extrapolation, the scale factor, $f_{\rm scale}$, is given by $\frac{\mathcal{L}_\Upsilon}{\mathcal{L}_{\rm con}}\frac{\sigma_\Upsilon}{\sigma_{\rm con}}\frac{\epsilon_\Upsilon}{\epsilon_{\rm con}}$, where $\frac{\mathcal{L}_\Upsilon}{\mathcal{L}_{\rm con}}$, $\frac{\sigma_\Upsilon}{\sigma_{\rm con}}$, and $\frac{\epsilon_\Upsilon}{\epsilon_{\rm con}}$ are the ratios of luminosity, cross sections, and efficiencies at the bottomonium masses and continuum energy points. The $s$ dependence of the cross section is assumed to be $1/s$ [15] and the corresponding scale factor is 0.079 for the $\Upsilon(1S)$ and 0.30 for the $\Upsilon(2S)$.

An unbinned simultaneous likelihood fit to the mass distributions is applied to extract the signal and background yields in the $\Upsilon(1S)$ and continuum data samples and in the $\Upsilon(2S)$ and continuum data samples. The signal shapes are obtained from MC simulations. In this fit, a second-order Chebyshev polynomial background shape is used for the $\Upsilon(1S)/\Upsilon(2S)$ decay backgrounds in addition to the normalized continuum contribution. The fit ranges and results for the $K^+K^-$, $\pi^+\pi^-\pi^0$, and $K^+\pi^-$ mass spectra are shown in Fig. 2 and Table I.

We determine a Bayesian 90% confidence level (C.L.) upper limit on $N^{\rm sig}$ by finding the value $N^{\rm UP}_{\rm sig}$ such that $\frac{\int_0^{N^{\rm UP}_{\rm sig}}\mathcal{L}dN^{\rm sig}}{\int_0^{\infty}\mathcal{L}dN^{\rm sig}} = 0.90$, where $N_{\rm sig}$ is the number of signal events and $\mathcal{L}$ is the value of the likelihood as a function of $N_{\rm sig}$. The statistical significance of the signal is estimated from the difference of the logarithmic likelihoods, $-2\ln(\mathcal{L}_0/\mathcal{L}_{\rm max})$, taking into account the difference in the number of degrees of freedom in the fits, where $\mathcal{L}_0$ and $\mathcal{L}_{\rm max}$ are the likelihoods of the fits without and with signal, respectively.

After requiring $|M_{K^+K^-} - m_\phi| < 8$ MeV/$c^2$, $|M_{\pi^+\pi^-\pi^0} - m_\omega| < 30$ MeV/$c^2$, and $|M_{K^+\pi^-} - m_{K^{*0}(892)}|$ $<100$ MeV/$c^2$, which contain around 95% of the signal according to MC simulations, the Dalitz plots for the $\phi K^+K^-$, $\omega\pi^+\pi^-$, and $K^{*0}(892)K^-\pi^+$ final states are shown in Fig. 3, where $m_\phi$, $m_\omega$, and $m_{K^{*0}(892)}$ are the nominal $\phi$, $\omega$, and $K^{*0}(892)$ masses [1]. Interestingly, the events accumulate near the phase space boundary, reflecting the quasi-two-body nature of these decays.

To categorize the quasi-two-body decays into $VT$ or $AP$ final states, we further require the angle between $V$ and $T$ ($A$ and $P$) in the $e^+e^-$ C.M. frame to be greater than 179°

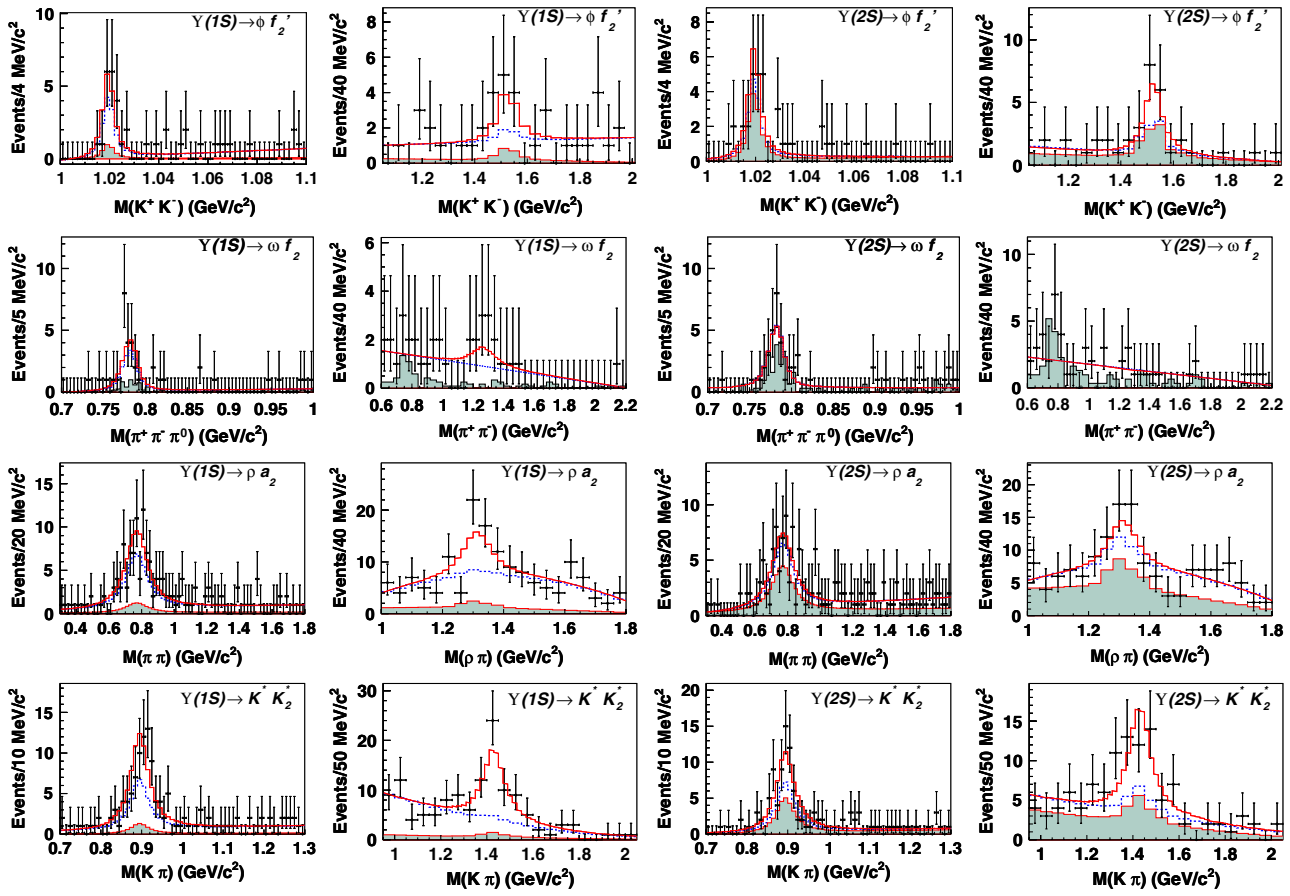


FIG. 4 (color online). The mass projections for the vector and tensor meson candidates from 2D fits to the events from $\Upsilon(1S)$ and $\Upsilon(2S)$ two-body decays ($VT$ modes). The open histograms show the results of the 2D simultaneous fits, the dotted curves show the total background estimates, and the shaded histograms are the normalized continuum contributions.

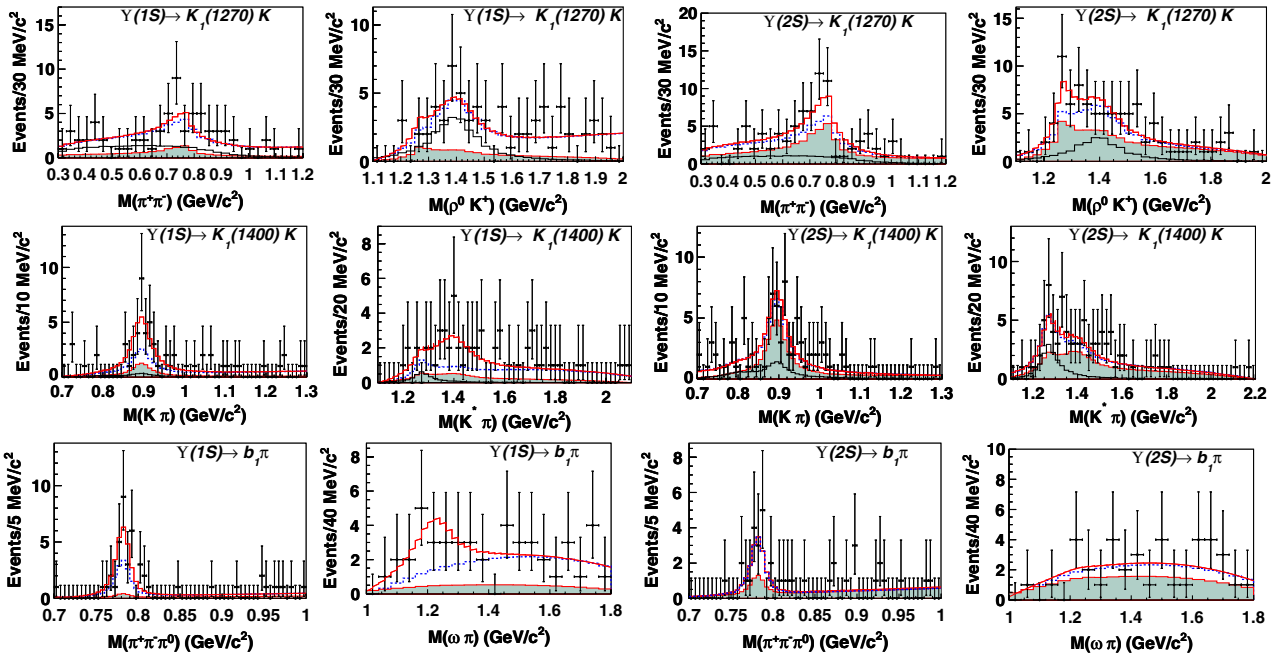


FIG. 5 (color online). The mass projections for the vector (from axial-vector decay) and axial-vector meson candidates from 2D fits to the events from $\Upsilon(1S)$ and $\Upsilon(2S)$ two-body decays ($AP$ modes). The open histograms show the results of the 2D simultaneous fits, the dotted curves show the total background estimates, the dot-dashed curves are the cross-feed backgrounds described in the text, and the shaded histograms are the normalized continuum contributions.

for the channels with a $\pi^0$, or 179.5° for the other channels. The combination with the minimum value of $\delta_{\min} = (M_1 - m_V)^2 + (M_2 - m_T)^2$ is selected as the $V$ and $T$ candidate, where $M_1$ and $M_2$ are the invariant masses of the $V$ and $T$ decay final-state particles, respectively. The same technique is used to select the best $AP$ candidate. This method introduces negligible bias in the meson pair selection according to MC simulation.

For the selected events, Fig. 4 shows the invariant-mass distributions for the vector and tensor meson candidates, and Fig. 5 shows the invariant-mass distributions for the vector (from axial-vector decay) and axial-vector meson candidates for $\Upsilon(1S)$ and $\Upsilon(2S)$ two-body decays. We extend the unbinned simultaneous maximum likelihood fit described above for three-body decays into a two-dimensional (2D) fit. We assume the mass distributions of the $V$ and $T$ particles to be uncorrelated; thus, the mass distributions in the 2D space can be represented by the product of two one-dimensional (1D) probability density functions (pdf). The 2D fitting function is parameterized as

$$f(M_1, M_2) = N^{\rm sig} s_1(M_1) s_2(M_2) + N^{\rm bg}_{sb} s_1(M_1) b_2(M_2) + N^{\rm bg}_{bs} b_1(M_1) s_2(M_2) + N^{\rm bg}_{bb} b_1(M_1) b_2(M_2),$$

where $s_1(M_1)$ and $b_1(M_1)$ are the 1D signal and background pdfs for $V$, respectively, and $s_2(M_2)$ and $b_2(M_2)$ are the corresponding pdfs for $T$. Here, the free parameters are the signal yield $N^{\rm sig}$ and the background yields $N^{\rm bg}_{sb}$, $N^{\rm bg}_{bs}$, and $N^{\rm bg}_{bb}$. Similar 2D pdfs are used to fit the vector (in axial-vector decays) and axial-vector meson candidates for the $AP$ modes. In these fits, we assume there is no interference between the signal and other components due to the limited statistics. The 1D projections from the 2D fits are shown in Figs. 4 and 5 with the contribution from each component indicated. In the fits to the $K_1(1270)^+K^-$ and $K_1(1400)^+K^-$ modes, the cross-feed background components from $K_1(1400)^+K^- \to K^{*0}K^-\pi^+$ and $K_1(1270)^+K^- \to \rho^0 K^+ K^-$ are also included and shown as dot-dashed lines. The fit results are shown in Table I.

There are several sources of systematic errors for the branching fraction measurements. The uncertainty in the tracking efficiency for tracks with angles and momenta characteristic of signal events is about 0.35% per track and is additive. The uncertainty due to particle identification efficiency is 1% with an efficiency correction factor of 0.97 for each pion and 0.8% with an efficiency correction factor 0.97 for each kaon, respectively. The uncertainty in selecting $\pi^0$ candidates is estimated by comparing control samples of $\eta \to \pi^0\pi^0\pi^0$ and $\eta \to \pi^+\pi^-\pi^0$ decays in data and amounts to 3.7%. Errors on the branching fractions of the intermediate states are taken from the PDG listings [1]. According to MC simulation, the trigger efficiency is greater than 99%, so that the corresponding uncertainty can be neglected. We estimate the systematic errors associated with the fitting procedure by changing the order of the background polynomial and the range of the fit; the differences in the fitted results, which are 1.3%–29% depending on the final-state particles that are

taken as systematic errors. We estimate the systematic errors associated with the resonance parameters by changing the values of the masses and widths of the resonances by $\pm 1\sigma$; the differences of 0.6%–7.3% in the fitted results are taken as systematic errors. For the central values of the branching fractions, the average difference between alternative C.M. energy dependences of the cross section is included as a systematic error due to the uncertainty of the continuum contribution, which is in the range of 4.2% to 22%. The uncertainty due to limited MC statistics is at most 0.5%. Finally, the uncertainties on the total numbers of $\Upsilon(1S)$ and $\Upsilon(2S)$ events are 2.2% and 2.3%, respectively. Assuming that all of these systematic error sources are independent, the total systematic error is 11%–31% depending on the final state.

Table I shows the results for the branching fractions including the upper limits at 90% C.L. for the channels with a statistical significance less than $3\sigma$. The corresponding ratio of the branching fractions of $\Upsilon(2S)$ and $\Upsilon(1S)$ decay is calculated; in some cases, the systematic errors cancel. In order to set conservative upper limits on these branching fractions, the efficiencies are lowered by a factor of $1 - \sigma_{\rm sys}$ in the calculation, where $\sigma_{\rm sys}$ is the total systematic error. All the results on the branching fractions, including upper limits, are below CLEO's preliminary results [3].

In summary, we have measured $\Upsilon(1S)$ and $\Upsilon(2S)$ hadronic exclusive decays to three-body final states and two-body processes. Signals are observed for the first time in the $\Upsilon(1S) \to \phi K^+K^-, \omega\pi^+\pi^-, K^{*0}K^-\pi^+, K^{*0}K_2^{*0}$ and $\Upsilon(2S) \to \phi K^+K^-$, $K^{*0}K^-\pi^+$ decay modes. Besides $K^{*0}K_2^{*0}$, no other two-body processes are observed in all investigated final states. We find that for the processes $\phi K^+K^-$, $K^{*0}K^-\pi^+$, and $K^{*0}\bar{K}_2^{*0}(1430)$, the $Q_{\rm Y}$ ratios are consistent with the expected value, while for $\omega\pi^+\pi^-$, the measured $Q_{\rm Y}$ ratio is $2.6\sigma$ below the pQCD expectation. The results for the other modes are inconclusive due to low statistical significance. These results may supply useful guidance for interpreting violations of the 12% rule for OZI-suppressed decays in the charmonium sector.

We thank the KEKB group for excellent operation of the accelerator; the KEK cryogenics group for efficient solenoid operations; and the KEK computer group, the NII, and PNNL/EMSL for valuable computing and SINET4 network support. We acknowledge support from MEXT, JSPS and Nagoya's TLPRC (Japan); ARC and DIISR (Australia); NSFC (China); MSMT (Czechia); DST (India); INFN (Italy); MEST, NRF, GSDC of KISTI, and WCU (Korea); MNiSW (Poland); MES and RFAAE (Russia); ARRS (Slovenia); SNSF (Switzerland); NSC and MOE (Taiwan); and DOE and NSF (USA).

[1] K. Nakamura *et al.* (Particle Data Group), J. Phys. G **37**, 075021 (2010) and 2011 partial update for the 2012 edition.

[2] D. Besson *et al.* (CLEO Collaboration), Phys. Rev. D **74**, 012003 (2006).

[3] Some preliminary results on two-body hadronic decays can be found in: S. A. Dytman *et al.* (CLEO Collaboration) arXiv:hep-ex/0307035.

[4] S. Okubo, Phys. Lett. **5**, 165 (1963); G. Zweig, CERN Report Nos. Th 401 and 412, 1964; J. Iizuka, K. Okada, and O. Shito, Prog. Theor. Phys. **35**, 1061 (1966); J. Iizuka, Prog. Theor. Phys. Suppl. **37**, 21 (1966).

[5] T. Appelquist and H. D. Politzer, Phys. Rev. Lett. **34**, 43 (1975); A. De Rújula and S. L. Glashow, Phys. Rev. Lett. **34**, 46 (1975); M. E. B. Franklin *et al.*, Phys. Rev. Lett. **51**, 963 (1983); Y. F. Gu and X. H. Li, Phys. Rev. D **63**, 114019 (2001).

[6] For recent reviews, please see X. H. Mo, C. Z. Yuan, and P. Wang, High Energy Phys. Nucl. Phys. **31**, 686 (2007); N. Brambilla *et al.*, Eur. Phys. J. C **71**, 1 (2011).

[7] Charge-conjugate decays are implicitly assumed throughout the paper.

[8] A. Abashian *et al.* (Belle Collaboration), Nucl. Instrum. Methods Phys. Res., Sect. A **479**, 117 (2002).

[9] S. Kurokawa and E. Kikutani, Nucl. Instrum. Methods Phys. Res., Sect. A **499**, 1 (2003), and other papers included in this volume.

[10] D. J. Lange, Nucl. Instrum. Methods Phys. Res., Sect. A **462**, 152 (2001).

[11] Y. Tosa, Report No. DPNU-34-1976.

[12] T. Sjöstrand, S. Mrenna, and P. Skands, J. High Energy Phys. 05 (2006) 026.

[13] E. Nakano, Nucl. Instrum. Methods Phys. Res., Sect. A **494**, 402 (2002).

[14] A. Abashian *et al.*, Nucl. Instrum. Methods Phys. Res., Sect. A **491**, 69 (2002).

[15] The dependence of the cross section on the beam energy could vary from $1/s$ to $1/s^4$, which is included as a source of systematic error.